

# Supplemental Material

## **Primitive to conventional geometry projection for efficient phonon transport calculations**

Xun Li<sup>1</sup>, Simon Thébaud<sup>2</sup>, and Lucas Lindsay<sup>1†</sup>

<sup>1</sup>*Materials Science and Technology Division, Oak Ridge National Laboratory, Oak Ridge, Tennessee  
37831, USA*

<sup>2</sup>Univ Rennes, INSA Rennes, CNRS, Institut FOTON-UMR 6082, F-35000 Rennes, France

Corresponding email: [lindsaylr@ornl.gov](mailto:lindsaylr@ornl.gov)<sup>†</sup>

## Supplementary Notes

### Supplementary Note 1. Derivation of Eq. 1 in the main text

In PTS dynamics, the atom  $K$  in the conventional cell  $p$  labeled as  $pK$  is changed to label  $hpk$  where  $h$  is the atom's layer and  $k$  is the atom index in that layer. The harmonic IFCs between atom  $K$  in the original conventional cell and  $K'$  in the  $p'$  cell are then relabeled:  $\Phi_{\alpha\beta}^{0K,p'K'} = \Phi_{\alpha\beta}^{h0k,h'p'k'}$ . Now choosing the first layer ( $h = 0$ ) as the new primitive basis, only  $\Phi_{\alpha\beta}^{00k,h'p'k'}$  is needed. The lattice vectors in the new basis are then  $\mathbf{R}_{p'} \rightarrow (\mathbf{R}_{p'} + h'\mathbf{S})$  with a phase of  $\frac{2\pi h'}{N}$ . Accordingly, the wavevectors are labeled with an integer  $l$  representing the phase degree of freedom:  $\mathbf{q} \rightarrow (\mathbf{q}, l)$ . Replacing the terms in the conventional formula of the dynamical matrix

$$D_{\alpha\beta}^{KK'}(\mathbf{q}) = \frac{1}{\sqrt{m_K m_{K'}}} \sum_{p'} \Phi_{\alpha\beta}^{0K,p'K'} e^{i\mathbf{q}\cdot\mathbf{R}_{p'}} \quad (1)$$

with PTS notations, we obtain:

$$D_{\alpha\beta}^{kk'}(\mathbf{q}, l) = \frac{1}{\sqrt{m_k m_{k'}}} \sum_{h'p'} \Phi_{\alpha\beta}^{00k,h'p'k'} e^{i\mathbf{q}\cdot(\mathbf{R}_{p'}+h'\mathbf{S})} e^{i2\pi lh'/N} \quad (2)$$

which is Eq. (1) in the main text.

### Supplementary Note 2. Details of calculations for a large toy system

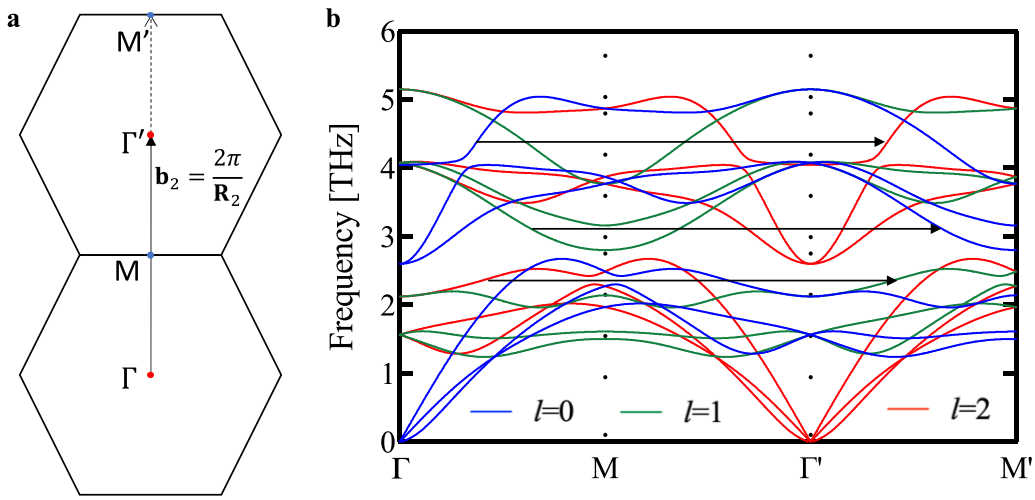
Our goal here is to test the PTS transport formalism on a larger test system without incurring needless computational cost from new DFT supercell calculations. To this end, the 6-atom GeTe conventional cell is expanded to a  $4 \times 4 \times 1$  supercell to create a new 96-atom conventional unit cell with 32 atoms (16 Ge and 16 Te) in each layer (primitive basis). The harmonic and anharmonic interatomic force constants of the original GeTe system were mapped to the new unit cell. We then changed the mass of each atom so that it is a new material system rather than a GeTe superlattice. The mass of each atom is calculated as

$$m_K^n = m_0^n * \left(1 - \frac{K-1}{16}\right) \quad (3)$$

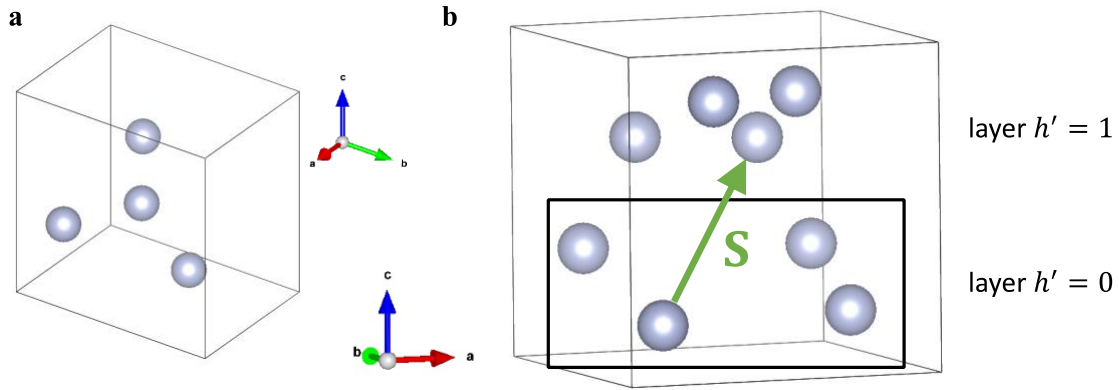
where  $m_0$  is the naturally occurring atomic mass,  $m_i$  is the atomic mass for atom index  $K$  in the conventional cell, and superscript  $n$  represents Ge or Te. Supplementary Figure 7 shows the dispersions for the toy system. The dispersions calculated from conventional and PTS methods

overlap. The PTS dynamics on this larger system gives identical thermal conductivity values as those from the conventional cell with a computational speedup  $\sim 9$ , agreeing with the expected  $1/N^2$  ratio where  $N=3$ . Specifically, for a  $q$  mesh of  $2 \times 2 \times 3$  the cpu hours for the calculations are 10.67 (PTS) and 80.46 (conventional). For a  $q$  mesh of  $3 \times 3 \times 5$ , the cpu hours are 78.99 (PTS) and 678.93 (conventional).

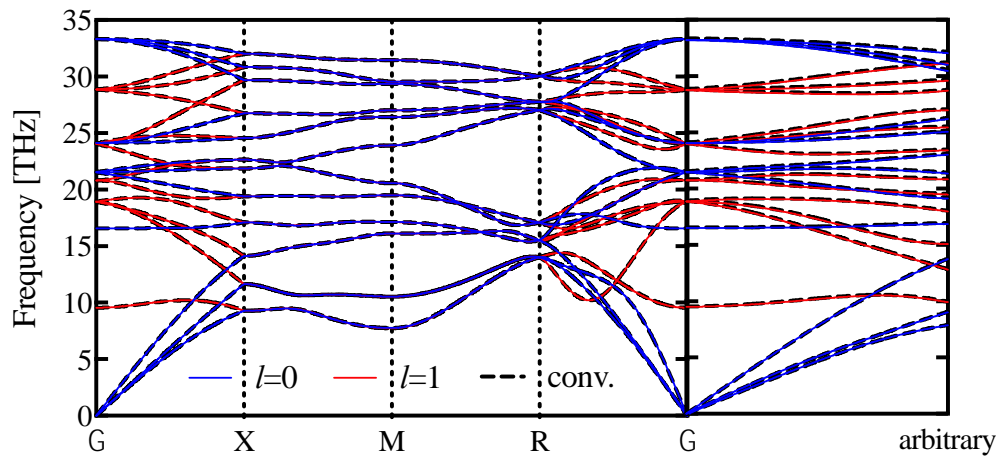
### Supplemental figures



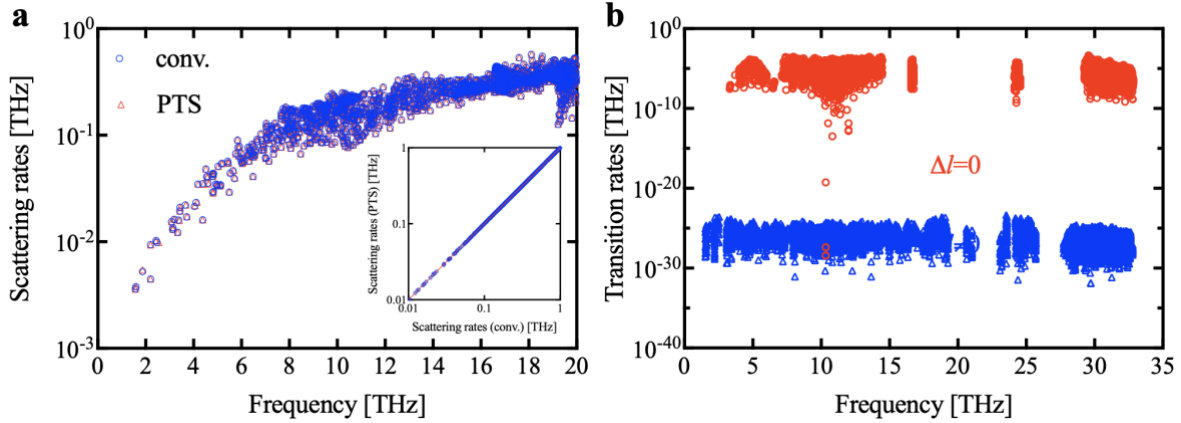
Supplementary Figure 1 Phonon dispersion of GeTe across two Brillouin zones. **a** The path  $\Gamma \rightarrow M \rightarrow \Gamma' \rightarrow M'$  in reciprocal space. **b** Phonon dispersion along the path in **a**. Here,  $n_x = 2$ ,  $n_y = 1$ , and  $n_z = 1$ . Going from  $\Gamma \rightarrow M$  to  $\Gamma' \rightarrow M'$  requires  $\Delta \mathbf{q} = \left[0, \frac{2\pi}{R_2}, 0\right]$  with  $g_1 = 0$ ,  $g_2 = 1$ , and  $g_3 = 0$ . Equation (18) in the main text gives  $\Delta l = -1$ , which is verified in Supplementary Figure 1b where phonon dispersions for the two paths are compared. Note that  $l=-1$  is equivalent to  $l=2$ .



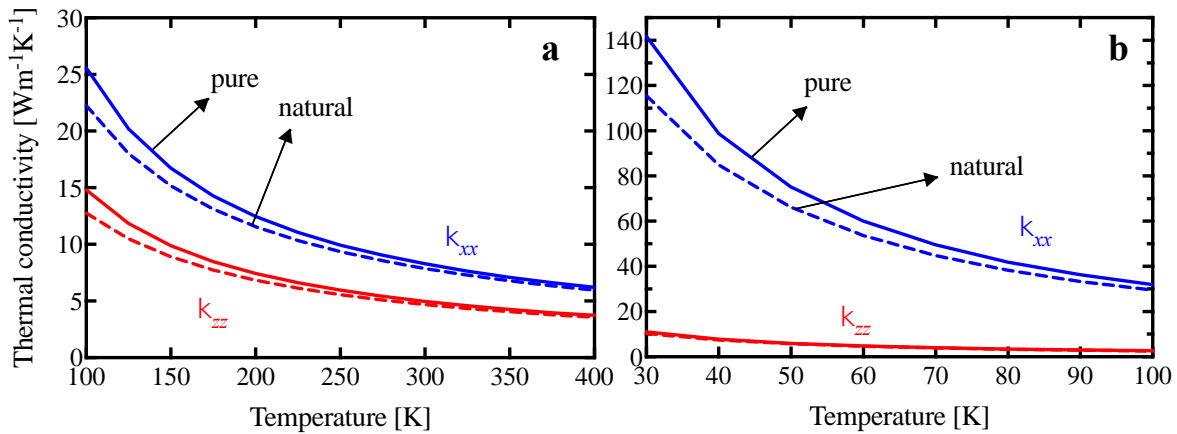
Supplementary Figure 2 Crystal structure of solid N<sub>2</sub> (I213 space group). **a** Primitive unit cell with 4 atoms. The angle between pairs of lattice vectors is 109.47°. **b** Conventional unit cell with 8 atoms in 2 layers related by translation vector **S** (green arrows). The angle between pairs of lattice vectors is 90°. The black rectangle highlights that a single layer can be used to describe the dynamics in a conventional unit cell.



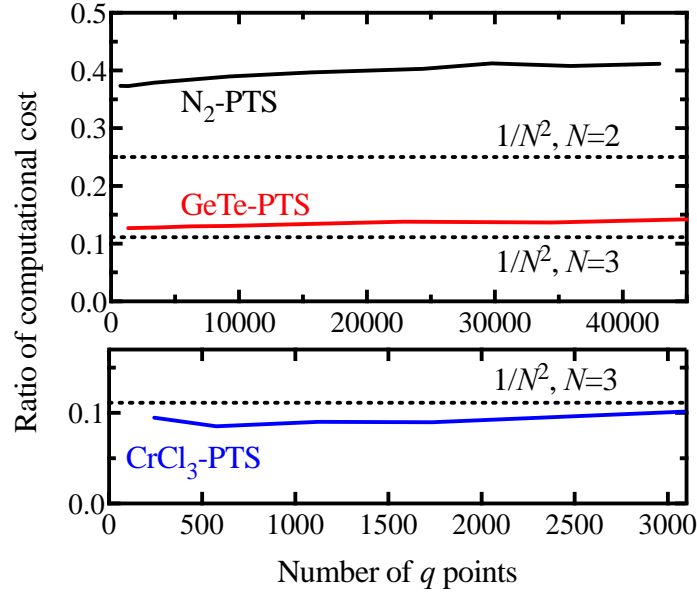
Supplementary Figure 3 Comparison of phonon dispersions of solid N<sub>2</sub> from conventional dynamics (underlying black dashed curves) and PTS dynamics (colored solid curves) along high-symmetry lines and an arbitrary direction from the  $\Gamma$  point to  $(q_x = 0.123\pi/a, q_y = 0.456\pi/b, q_z = 0.789\pi/c)$ . Blue and red solid curves correspond to integers *l*=0 and *l*=1, respectively.



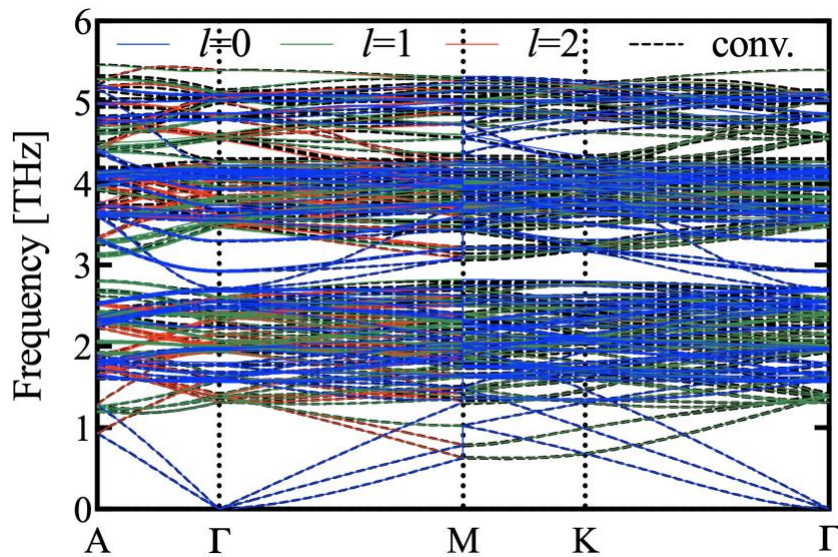
Supplementary Figure 4 Total scattering and individual transition rates for phonons in solid  $N_2$ . **a** Scattering rates as a function of phonon frequency from separate conventional (blue) and PTS (red) dynamics. Inset: Direct comparison of scattering rates from the two methods. The red solid line is a guide for the eye showing equality. **b** Individual anharmonic phonon transition rates for a phonon mode at the  $\Gamma$  point with  $(\omega=21.54 \text{ THz}, j=7)$  as a function of the frequency of one of the other interacting modes in three-phonon interactions. Transition rates with  $\Delta l \neq 0$ , i.e., violating conservation of  $l$ , are numerically zero.



Supplementary Figure 5 Anisotropic thermal conductivity of **a** GeTe and **b**  $CrCl_3$ . Thermal conductivities for naturally occurring samples are smaller than those for pure samples due to phonon-isotope scattering.



Supplementary Figure 6 Ratio of computational cost for thermal conductivity calculations of  $N_2$  (black curve), GeTe (red curve), and  $CrCl_3$  (blue curve) as a function of  $q$  mesh density. The dotted lines correspond to  $1/N^2$  values where  $N$  is 2 and 3. The computational saving approaches the  $1/N^2$  as the material system becomes more complex.



Supplementary Figure 7 Comparison of phonon dispersions of a large GeTe toy system from conventional dynamics (black dashed curves) and PTS dynamics (colored solid curves) along high-symmetry lines. Blue, green, and red solid curves correspond to integers  $l=0$ ,  $l=1$ , and  $l=2$ , respectively.